The Binary Phase-Shift Keyed Bit-Error Performance Under an In-Band Pulsed-Chirp Radio Frequency Interference

H. Tsou,[1] J. Gin,[1] C. Wang,[1] and M. Sue[1]

The impact of an in-band pulsed-chirp radio frequency interference (RFI) on the coherent reception of a fully suppressed binary phase-shift keying (BPSK) signal was analyzed. To better understand the impact from the pulsed nature of the RFI, two scenarios were studied separately—one for low-rate and the other for high-rate telemetry, depending upon whether the symbol rate of the BPSK signal was lower or higher, respectively, than the pulse repetition frequency (PRF) of the RFI. For each case, the bit-error rate (BER) was derived as a function of various RFI parameters after analyzing the RFI-impacted carrier tracking and symbol detection of the coherent receiver. The analytical models resulting from this study are useful in assessing the BER performance degradation for BPSK signals against a set of pulsed-chirp RFI parameters.

I. Introduction

A proposed synthetic aperture radar project is to operate near one of the Deep Space Network (DSN) complexes. This raises concerns about potential interference to the DSN operations because the radar pulse is much stronger than the DSN's downlink telemetry and it sweeps across a wide band that, in some of the proposed operation modes, may encompass the DSN band in its entirety, rendering an in-band radio frequency interference (RFI) that will adversely affect the DSN downlink. With the assumption that the in-band RFI is not saturating the receiver front-end, this study was set to assess the degradation of the bit-error rate (BER) performance by analyzing the carrier tracking and symbol detection performance based upon the following specifications for the pulsed-chirp radar signal:

(1) Peak pulse effective isotropic radiated power (EIRP): 30 to 40 dBW

(2) Pulse repetition rate (PRF): 1 to 4 kHz

(3) Pulse duration (τ): 50 to 400 μs

[1] Communications Architectures and Research Section.

The research described in this publication was carried out by the Jet Propulsion Laboratory, California Institute of Technology, under a contract with the National Aeronautics and Space Administration.

(4) Duty factor (d): 20 to 40 percent

(5) Frequency sweeping rate (β): 0.5 to 1 MHz/μs

(6) Chirp bandwidth: 25 to 400 MHz

In this study, two scenarios were investigated separately—one for low-rate DSN missions in which the ratio of the radar pulse duration,

$$\tau = \frac{d}{\mathrm{PRF}} \tag{1}$$

to the telemetry symbol duration, T, is much smaller than one, and the other for high-rate DSN missions in which the ratio is much larger than one. From the viewpoint of a carrier tracking loop in the low-rate case, a large number of radar pulses will be seen within the loop's time constant, which is commonly referred to as the reciprocal of the loop's one-sided bandwidth (B_L), since $B_L T \ll 1$ holds for a well-designed loop. In such a case, the pulsed RFI is effectively time-averaged by the loop, rendering an interference behaving just like a non-pulsed background noise that contributes to the receiver no more than a decrease of the loop signal-to-noise ratio (SNR). Contrarily, the pulsed nature of the RFI remains intact in the high-rate case since the loop's time constant covers no more than a few radar pulses. This poses a greater threat to the coherent receiver operation since the carrier tracking loop may be abruptly disturbed by a short but fairly strong radar pulse and lose its lock in the middle of tracking.

In addition to the impact from increased phase noise of carrier tracking, the BER performance in both cases is seen to degrade further as a bias introduced by the RFI to the receiver's symbol detection filter output causes more erroneous hard-decisions. In the following, the analytical models of the carrier tracking with the Costas loop for binary phase-shift keyed (BPSK) signals and symbol decision will be presented for both low-rate and high-rate cases. They are followed by a discussion of the worst-case BER performance under several operational scenarios. In the end, a recommendation is given based upon the numerical results obtained from both the analytical models and the software simulations.

II. Mathematical Model—Low-Rate Telemetry

A. Signals

For the low-rate case, it is assumed that the symbol interval of the DSN downlink telemetry contains multiple chirp radar pulses such that

$$\lfloor T(\mathrm{PRF}) \rfloor > 1 \tag{2}$$

With a peak radar power α times as strong as the desired signal, the received signal, in its complex equivalent form, is modeled as a sum of a phase-shift-keyed (PSK) telemetry signal, a complex white Gaussian noise $n(t)$, and a stream of chirp radar pulses as below:

$$\begin{aligned} r(t) = {} & \sqrt{P_d}\exp\left\{i\big(2\pi f_c t + \theta_d(t) + \theta_c\big)\right\} + n(t) \\ & + \sqrt{\alpha P_d}\exp\left\{i\big(2\pi(f_c+\Delta f)t + \theta_c + \Delta\theta\big)\right\} \\ & \times \sum_l \exp\left\{i\pi\beta\left(t - \frac{\tau}{2} - \Gamma - \frac{l}{\mathrm{PRF}}\right)^2\right\} \mathrm{rect}\left(\frac{t - \tau/2 - \Gamma - l/\mathrm{PRF}}{\tau}\right) \end{aligned} \tag{3}$$

where P_d is the power of the desired telemetry, f_c is the downlink carrier frequency, $\Delta f = f_i - f_c$ is the carrier frequency separation and $\Delta\theta$ is a uniformly distributed random phase between the carriers as $t = 0$, Γ is a random time offset uniformly distributed over a pulse repetition cycle, and $\theta_d(t)$ is the phase profile of the PSK signal as

$$\theta_d(t) = \sum_k \theta_k \text{ rect}\left\{\frac{t - kT - T/2}{T}\right\} \tag{4}$$

where θ_k takes one of the pre-set phase values to represent the kth symbol of the PSK signal and

$$\text{rect}(x) \triangleq \begin{cases} 1, & |x| \le \frac{1}{2} \\ 0, & \text{elsewhere} \end{cases}$$

After mixing the received signal with a locally generated carrier reference, the output of the phase detector (mixer) becomes

$$\begin{aligned} r(t)\exp\left\{-i\left(2\pi\hat{f}_c t + \hat{\theta}_c\right)\right\} = {} & \sqrt{P_d}\exp\left\{i\big(2\pi\Delta f_c t + \theta_d(t) + \phi_c\big)\right\} + n'(t) \\ & + \sqrt{\alpha P_d}\exp\left\{i\big(2\pi\left(\Delta f_c + \Delta f\right)t + \phi_c + \Delta\theta\big)\right\} \\ & \times \sum_l \exp\left\{i\pi\beta\left(t - \frac{\tau}{2} - \Gamma - \frac{l}{\text{PRF}}\right)^2\right\} \text{rect}\left(\frac{t - \tau/2 - \Gamma - l/\text{PRF}}{\tau}\right) \end{aligned} \tag{5}$$

where $\phi_c = \theta_c - \hat{\theta}_c$ is the phase error to be tracked by the carrier tracking loop. When perfect carrier frequency and symbol-timing references are established, the integrate-and-dump filter output for the kth symbol that, as assumed, contains a stream of full radar cycles[2] (namely, $T(\text{PRF}) = L \in \mathbb{N}$) is obtained, in its complex-valued form, as

$$\begin{aligned} & I_k + iQ_k \\ & = \sqrt{P_d}T\exp\left\{i\left(\theta_k + \phi_c\right)\right\} \\ & \quad + \sqrt{\frac{\alpha P_d}{2\beta}\left\{\left[C\left(z_1\right) + C\left(z_2\right)\right]^2 + \left[S\left(z_1\right) + S\left(z_2\right)\right]^2\right\}}\exp\left\{i\left(\phi_c + \lambda + \eta\right)\right\}\sum_{l=0}^{L-1}\exp\left\{i2\pi l\left(\frac{\Delta f}{\text{PRF}}\right)\right\} \\ & \quad + N_I + iN_Q \end{aligned} \tag{6}$$

by integrating Eq. (5) from kT to $(k+1)T$. Here,

[2] This is assumed for simplicity to avoid the situation in which some radar pulses may sit across a symbol boundary.

$$C(x) \triangleq \int_0^x \cos\left(\frac{\pi}{2}t^2\right) dt$$
$$S(x) \triangleq \int_0^x \sin\left(\frac{\pi}{2}t^2\right) dt \tag{7}$$

are the Fresnel cosine and sine integrals, respectively. The upper limits for these integrals in Eq. (6) are

$$z_1 = \tau\sqrt{\frac{\beta}{2}}\left[1 + \frac{2\Delta f}{\beta\tau}\right]$$
$$z_2 = \tau\sqrt{\frac{\beta}{2}}\left[1 - \frac{2\Delta f}{\beta\tau}\right] \tag{8}$$

and the phases λ and η are defined as

$$\lambda = 2\pi\Delta f\left(kT + \frac{\tau}{2} - \frac{\Delta f}{2\beta}\right) + \Delta\theta \tag{9}$$

and

$$\eta = \tan^{-1}\left(\frac{S(z_1) + S(z_2)}{C(z_1) + C(z_2)}\right) \triangleq \tan^{-1}\left(\frac{S_z}{C_z}\right) \tag{10}$$

where

$$C_z = \frac{C(z_1) + C(z_2)}{2}$$
$$S_z = \frac{S(z_1) + S(z_2)}{2} \tag{11}$$

By defining

$$Z(\Delta f) \triangleq \sum_{l=0}^{L-1} \exp\left\{i2\pi l\left(\frac{\Delta f}{\mathrm{PRF}}\right)\right\} = \begin{cases} L, & \text{when } (\Delta f/\mathrm{PRF}) \in \mathbb{Z} \\ \dfrac{1 - e^{i2\pi\Delta f T}}{1 - e^{i2\pi\Delta f/\mathrm{PRF}}}, & \text{when } (\Delta f/\mathrm{PRF}) \notin \mathbb{Z} \end{cases} \tag{12}$$

the output of the integrate-and-dump (arm) filters is found from Eq. (6) as

$$I_k = \sqrt{P_d}T\cos(\theta_k + \phi_c) + \sqrt{\frac{2\alpha P_d}{\beta}}\left[A_z\cos(\phi_c + \lambda) - B_z\sin(\phi_c + \lambda)\right] + N_I$$
$$Q_k = \sqrt{P_d}T\sin(\theta_k + \phi_c) + \sqrt{\frac{2\alpha P_d}{\beta}}\left[A_z\sin(\phi_c + \lambda) + B_z\cos(\phi_c + \lambda)\right] + N_Q \tag{13}$$

where

$$\begin{aligned} A_z &= \mathrm{Re}\big[Z\left(\Delta f\right)\big]C_z - \mathrm{Im}\big[Z\left(\Delta f\right)\big]S_z \\ B_z &= \mathrm{Re}\big[Z\left(\Delta f\right)\big]S_z + \mathrm{Im}\big[Z\left(\Delta f\right)\big]C_z \end{aligned} \tag{14}$$

B. Carrier Tracking

To track a fully suppressed BPSK signal (namely, $\theta_k = 0$ or π such that $\cos\theta_k = d_k \in \{\pm 1\}$), a Costas loop would produce a normalized error feedback signal,

$$e_k = \frac{I_k Q_k}{P_d T^2} = \frac{1}{2}\sin(2\phi_c) + \frac{\alpha}{\beta T^2}\left\{\left(A_z^2 - B_z^2\right)\sin\left[2\left(\phi_c + \lambda\right)\right] + 2A_z B_z \cos\left[2\left(\phi_c + \lambda\right)\right]\right\} + N_e + N_{s,k} \tag{15}$$

where

$$N_e = \sqrt{\frac{2\alpha}{\beta T^2}}\left\{\left[N_1 B_z + N_2 A_z\right]\cos\left(\phi_c + \lambda\right) + \left[N_1 A_z - N_2 B_z\right]\sin\left(\phi_c + \lambda\right)\right\} + N_1 N_2 \tag{16}$$

is the contribution from the additive white Gaussian noise (AWGN) and

$$N_{s,k} = d_k\left\{N_1\sin\phi_c + N_2\cos\phi_c + \sqrt{\frac{2\alpha}{\beta T^2}}\left[A_z\sin\left(2\phi_c + \lambda\right) + B_z\cos\left(2\phi_c + \lambda\right)\right]\right\} \tag{17}$$

is the self-noise related to the transmitted symbol, with

$$\begin{aligned} N_1 &\triangleq \frac{N_I}{\sqrt{P_d}T} \\ N_2 &\triangleq \frac{N_Q}{\sqrt{P_d}T} \end{aligned} \tag{18}$$

such that

$$\sigma^2 = \sigma_{N_1}^2 = \sigma_{N_2}^2 = \frac{1}{2(E_b/N_0)} \tag{19}$$

where N_0 is the two-sided power spectral density of the complex white Gaussian noise. Note here that both N_e and $N_{s,k}$ are zero-mean. Thus, the deterministic part of the error feedback signal, Eq. (15), known as the S-curve of a tracking loop, is found as

$$SC\left(\phi_c\,|\lambda\right) = \frac{1}{2}\sin\left(2\phi_c\right) + \frac{\alpha}{\beta T^2}\left\{\left(A_z^2 - B_z^2\right)\sin\left[2\left(\phi_c + \lambda\right)\right] + 2A_z B_z\cos\left[2\left(\phi_c + \lambda\right)\right]\right\} \tag{20}$$

Equating Eq. (20) to zero and solving for ϕ_c leads to a steady-state carrier phase lock point,

$$\phi_0 = -\frac{1}{2}\tan^{-1}\left[\frac{\frac{2\alpha}{\beta T^2}\left(A_z^2+B_z^2\right)\sin\left[2\left(\xi+\lambda\right)\right]}{1+\frac{2\alpha}{\beta T^2}\left(A_z^2+B_z^2\right)\cos\left[2\left(\xi+\lambda\right)\right]}\right] \tag{21}$$

that shows a deviation from the ideal lock point at $\phi_0 = 0$. Here,

$$\xi = \tan^{-1}\left(\frac{B_z}{A_z}\right) \tag{22}$$

It also can be shown that the slope of the S-curve at ϕ_0 given in Eq. (21) is

$$g_{SC} = \sqrt{1+\frac{4\alpha}{\beta T^2}\left(A_z^2+B_z^2\right)\cos\left[2\left(\xi+\lambda\right)\right]+\left(\frac{2\alpha}{\beta T^2}\left(A_z^2+B_z^2\right)\right)^2} \tag{23}$$

Hence, for linear analysis where $\phi_c \sim \phi_0$, the error feedback signal in Eq. (15) is approximated by

$$e_k \approx g_{SC}\left(\phi_c-\phi_0\right)+N_e+N_{s,k} \tag{24}$$

C. Symbol Detection

The detection of a received BPSK symbol is performed by making a hard decision on the output of the in-phase integrate-and-dump filter of the Costas loop. From Eq. (13), the normalized decision variable is

$$\begin{aligned}\frac{I_k}{\sqrt{P_d}T} &= d_k\cos(\phi_c)+\sqrt{\frac{2\alpha}{\beta T^2}}\left[A_z\cos\left(\phi_c+\lambda\right)-B_z\sin\left(\phi_c+\lambda\right)\right]+\frac{N_I}{\sqrt{P_d}T}\\ &\triangleq u_k\left(\phi_c\right)+\frac{N_I}{\sqrt{P_d}T}\end{aligned} \tag{25}$$

Thus, the bit-error probability (conditioned on λ) as a function of ϕ_c is derived as

$$\begin{aligned}P_b\left(\phi_c\,|\lambda\right) &= \frac{1}{2}P_r\left\{u_k\left(\phi_c\right)<0\,|d_k=1\right\}+\frac{1}{2}P_r\left\{u_k\left(\phi_c\right)\geq 0\,|d_k=-1\right\}\\ &= \frac{1}{4}\mathrm{erfc}\left\{\sqrt{\frac{E_b}{N_0}}\left(\cos\phi_c+\sqrt{\frac{2\alpha}{\beta T^2}}\left[A_z\cos\left(\phi_c+\lambda\right)-B_z\sin\left(\phi_c+\lambda\right)\right]\right)\right\}\\ &\quad+\frac{1}{4}\mathrm{erfc}\left\{\sqrt{\frac{E_b}{N_0}}\left(\cos\phi_c-\sqrt{\frac{2\alpha}{\beta T^2}}\left[A_z\cos\left(\phi_c+\lambda\right)-B_z\sin\left(\phi_c+\lambda\right)\right]\right)\right\}\end{aligned} \tag{26}$$

Here, the phase error can be modeled as a Tikhonov-distributed random variable with a probability density function [1]

$$p\left(\phi_c\,|\lambda\right) = \frac{\exp\left(\frac{\rho_{\phi_c}}{4}\cos\left[2\left(\phi_c-\phi_0\right)\right]\right)}{\pi \mathrm{I}_0\left(\frac{\rho_{\phi_c}}{4}\right)}, \quad |\phi_c| \le \frac{\pi}{2} \tag{27}$$

with a finite loop SNR that can be shown as

$$\rho_{\phi_c} = g_{SC}^2\left(\frac{E_b/N_0}{B_L T}S_L\right)\left\{1+S_L\psi\left[1+\left(\frac{E_b}{N_0}\right)\frac{\left(1-\psi^2\right)\left[1-\cos\left(2\left(\xi+\lambda\right)\right)\right]}{1+2\psi\cos\left(2\left(\xi+\lambda\right)\right)+\psi^2}\right]\right\}^{-1} \tag{28}$$

where $\psi = \left(2\alpha/\beta T^2\right)\left(A_z^2+B_z^2\right)$ and

$$S_L = \left(1+\frac{1}{2E_b/N_0}\right)^{-1} \tag{29}$$

is the squaring loss associated with the tracking of a BPSK Costas loop. Note that, in Eq. (28), the reduction of loop SNR caused by the time-averaged RFI is evident by the term enclosed in the pair of braces. This term, as a function of ψ, disappears as expected when $\alpha = 0$.

Finally, by averaging Eq. (26) over the probability density function of ϕ_c given in Eq. (27), the conditional BER is found as

$$P_{b|\lambda} = \int_{-\pi/2}^{\pi/2} P_b\left(\phi_c\,|\lambda\right) p\left(\phi_c\,|\lambda\right) d\phi_c \tag{30}$$

while the unconditioned BER is obtained as

$$P_b = \frac{1}{2\pi}\int_{-\pi}^{\pi} P_{b|\lambda}\, d\lambda \tag{31}$$

by averaging Eq. (30) over a uniformly distributed λ.

D. Worst-Case Carrier Frequency Separation

Before moving on to the model for high-rate telemetry, it is worth paying extra attention to the special case of $(\Delta f/\mathrm{PRF}) \in \mathbb{Z}$. It turns out that this is the worst case, in which the coherent reception suffers most due to the RFI. By rewriting Eq. (26) as

$$\begin{aligned} P_b(\phi_c\,|\lambda) = {} & \frac{1}{4}\mathrm{erfc}\left\{\sqrt{\frac{E_b}{N_0}}\left(\cos\phi_c+\sqrt{\frac{2\alpha}{\beta T^2}\left(A_z^2+B_z^2\right)}\cos\left(\phi_c+\lambda+\xi\right)\right)\right\} \\ & + \frac{1}{4}\mathrm{erfc}\left\{\sqrt{\frac{E_b}{N_0}}\left(\cos\phi_c-\sqrt{\frac{2\alpha}{\beta T^2}\left(A_z^2+B_z^2\right)}\cos\left(\phi_c+\lambda+\xi\right)\right)\right\} \end{aligned} \tag{32}$$

one can first argue that the term

$$A_z^2 + B_z^2 = |Z(\Delta f)|^2 \left(C_z^2 + S_z^2\right) \tag{33}$$

is reaching its maximum when $|Z(\Delta f)|$ is maximized with $(\Delta f/\mathrm{PRF}) \in \mathbb{Z}$. This, in turn, stretches the difference between the arguments of the complementary error functions in Eq. (32) to its largest value, making the bigger (dominant) one of the two complementary error functions even bigger. In this worst-case scenario, the conditional bit-error probability of Eq. (26) becomes

$$P_b(\phi_c|\lambda) = \frac{1}{4}\mathrm{erfc}\left\{\sqrt{\frac{E_b}{N_0}}\left(\cos\phi_c + \sqrt{\frac{2\alpha}{\beta}}\left(\frac{d}{\tau}\right)\left[C_z\cos(\phi_c+\lambda) - S_z\sin(\phi_c+\lambda)\right]\right)\right\}$$

$$+ \frac{1}{4}\mathrm{erfc}\left\{\sqrt{\frac{E_b}{N_0}}\left(\cos\phi_c - \sqrt{\frac{2\alpha}{\beta}}\left(\frac{d}{\tau}\right)\left[C_z\cos(\phi_c+\lambda) - S_z\sin(\phi_c+\lambda)\right]\right)\right\} \tag{34}$$

and

$$\psi = \frac{2\alpha}{\beta}\left(\frac{d}{\tau}\right)^2\left(C_z^2 + S_z^2\right) \tag{35}$$

should be plugged into Eq. (28). Figure 1 shows a set of BER curves with different $(\Delta f/\mathrm{PRF})$ ratios for 1-kb/s BPSK and a 35-dB peak interference-to-signal power ratio, revealing a more than 2-dB performance gap between the best and the worst cases at the BER level of 10^{-4}.

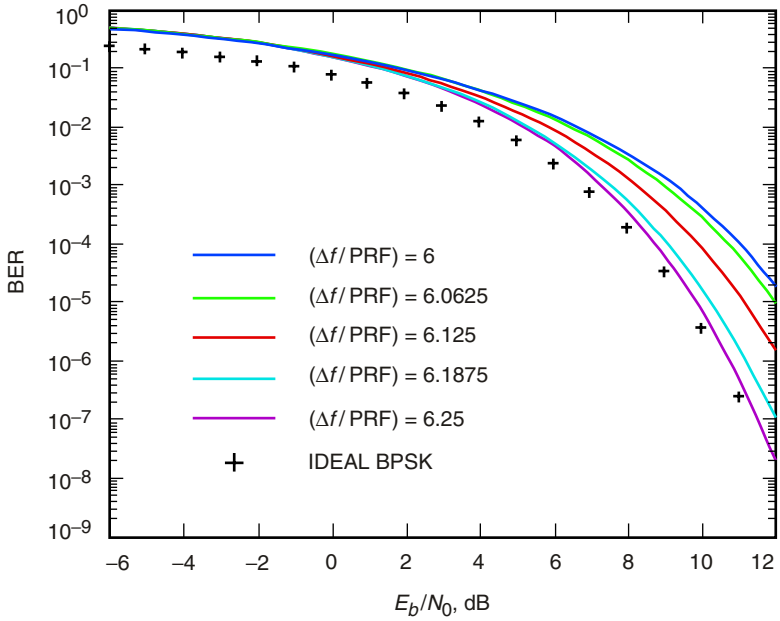

Fig. 1. BER curves for low-rate telemetry with different $(\Delta f/\mathrm{PRF})$ ratios.

III. Mathematical Model—High-Rate Telemetry

A. Signals

For this case, a chirp radar pulse will overlap a multiple of telemetry symbols transmitted at a higher rate than the PRF. One can model the complex equivalent signal at the receiver input as

$$r(t) = \sqrt{P_d}\exp\left\{i\big(2\pi f_c t + \theta_d(t) + \theta_c\big)\right\}$$
$$+ \sqrt{\alpha P_d}\exp\left\{i\big(2\pi(f_c+\Delta f)t + \pi\beta(t-\Gamma-\tau/2)^2 + (\theta_c+\Delta\theta)\big)\right\}\operatorname{rect}\left(\frac{t-\Gamma-\tau/2}{\tau}\right) + n(t) \quad (36)$$

Here, the radar pulse is defined in the time interval $[\Gamma, \Gamma+\tau)$, where Γ is a random time offset (uniformly distributed over a symbol duration) between the leading edges of the radar pulse and a telemetry symbol.

The phase detector (mixer) output becomes

$$r(t)\exp\left\{-i(2\pi\hat{f}_c t + \hat{\theta}_c)\right\} = \sqrt{P_d}\exp\left\{i\big(2\pi\Delta f_c t + \theta_d(t) + \phi_c\big)\right\}$$
$$+ \sqrt{\alpha P_d}\exp\left\{i\big(2\pi(\Delta f_c+\Delta f)t + \pi\beta(t-\Gamma-\tau/2)^2 + (\phi_c+\Delta\theta)\big)\right\}\operatorname{rect}\left(\frac{t-\Gamma-\tau/2}{\tau}\right) + n'(t) \quad (37)$$

Assuming perfect carrier frequency and symbol timing are established, the integrate-and-dump filter outputs associated with the kth symbol, which is assumed to stay fully within the chirp radar pulse, are

$$I_k = \sqrt{P_d}T\cos(\theta_k+\phi_c) + \sqrt{\frac{\alpha P_d}{2\beta}}\left\{\cos\phi_c\left[\hat{C}_k\cos\gamma - \hat{S}_k\sin\gamma\right] - \sin\phi_c\left[\hat{C}_k\sin\gamma + \hat{S}_k\cos\gamma\right]\right\} + N_I \quad (38)$$

$$Q_k = \sqrt{P_d}T\sin(\theta_k+\phi_c) + \sqrt{\frac{\alpha P_d}{2\beta}}\left\{\cos\phi_c\left[\hat{C}_k\sin\gamma + \hat{S}_k\cos\gamma\right] + \sin\phi_c\left[\hat{C}_k\cos\gamma - \hat{S}_k\sin\gamma\right]\right\} + N_Q$$

where

$$\gamma = 2\pi\Delta f\left(\Gamma + \frac{\tau}{2} - \frac{\Delta f}{2\beta}\right) + \Delta\theta \quad (39)$$

and

$$\hat{C}_k = C\left(\sqrt{2\beta}\left[(k+1)T - \left(\Gamma+\frac{\tau}{2}\right) + \frac{\Delta f}{\beta}\right]\right) - C\left(\sqrt{2\beta}\left[kT - \left(\Gamma+\frac{\tau}{2}\right) + \frac{\Delta f}{\beta}\right]\right)$$
$$\hat{S}_k = S\left(\sqrt{2\beta}\left[(k+1)T - \left(\Gamma+\frac{\tau}{2}\right) + \frac{\Delta f}{\beta}\right]\right) - S\left(\sqrt{2\beta}\left[kT - \left(\Gamma+\frac{\tau}{2}\right) + \frac{\Delta f}{\beta}\right]\right) \quad (40)$$

are differences of two Fresnel cosine integrals and two Fresnel sine integrals, both defined in Eq. (7). Here, in Eq. (38), the noise terms are zero-mean Gaussian random variables with variances

$$\sigma_{N_I}^2 = \sigma_{N_Q}^2 = \frac{N_0 T}{2} \tag{41}$$

B. Carrier Tracking

Similarly to the low-rate case, a Costas loop for BPSK signals produces the error feedback signal

$$e_k = \frac{I_k Q_k}{P_d T^2} = \frac{1}{2}\sin(2\phi_c) + \frac{\alpha}{2\beta T^2}\left[\left(\frac{\hat{C}_k^2 - \hat{S}_k^2}{2}\right)\sin(2\gamma) + \hat{C}_k\hat{S}_k\cos(2\gamma)\right]\cos(2\phi_c)$$

$$+ \frac{\alpha}{2\beta T^2}\left[\left(\frac{\hat{C}_k^2 - \hat{S}_k^2}{2}\right)\cos(2\gamma) - \hat{C}_k\hat{S}_k\sin(2\gamma)\right]\sin(2\phi_c) + N_{e,k} + N_{s,k} \tag{42}$$

where

$$N_{e,k} = N_1\sqrt{\frac{\alpha}{2\beta T^2}}\left(\left[\hat{C}_k\cos\gamma - \hat{S}_k\sin\gamma\right]\sin\phi_c + \left[\hat{C}_k\sin\gamma + \hat{S}_k\cos\gamma\right]\cos\phi_c\right)$$

$$+ N_2\sqrt{\frac{\alpha}{2\beta T^2}}\left(\left[\hat{C}_k\cos\gamma - \hat{S}_k\sin\gamma\right]\cos\phi_c - \left[\hat{C}_k\sin\gamma + \hat{S}_k\cos\gamma\right]\sin\phi_c\right) + N_1 N_2 \tag{43}$$

is the contribution from the AWGN noise and

$$N_{s,k} =$$

$$d_k\left(N_1\sin\phi_c + N_2\cos\phi_c + \sqrt{\frac{\alpha}{2\beta T^2}}\left(\left[\hat{C}_k\cos\gamma - \hat{S}_k\sin\gamma\right]\cos(2\phi_c) + \left[\hat{C}_k\sin\gamma + \hat{S}_k\cos\gamma\right]\sin(2\phi_c)\right)\right) \tag{44}$$

is the self-noise related to the transmitted symbol, with

$$\begin{aligned} N_1 &= \frac{N_I}{\sqrt{P_d}T} \\ N_2 &= \frac{N_Q}{\sqrt{P_d}T} \end{aligned} \tag{45}$$

such that

$$\sigma^2 = \sigma_{N_1}^2 = \sigma_{N_2}^2 = \frac{1}{2(E_b/N_0)} \tag{46}$$

Note here that both $N_{e,k}$ and $N_{s,k}$ are zero-mean. Thus, the deterministic part of the error feedback signal, Eq. (42), is found as

$$SC_k\left(\phi_c\,|\gamma\right) = \frac{1}{2}\sin\left(2\phi_c\right) + \frac{\alpha}{2\beta T^2}\left(\frac{\hat{C}_k^2 + \hat{S}_k^2}{2}\right)\sin\left[2\left(\phi_c + \gamma + \eta_k\right)\right] \tag{47}$$

where

$$\eta_k = \tan^{-1}\left(\frac{\hat{S}_k}{\hat{C}_k}\right) \tag{48}$$

Note here that Eq. (47) represents the "instantaneous" S-curve of the loop operation, which exists only for a loop with an infinitely large loop bandwidth or, equivalently, an infinitely small loop time constant. Equating $SC_k(\phi_c)$ in Eq. (47) to zero and solving for ϕ_c leads to an "instantaneous" carrier phase lock point,

$$\phi_{0,k} = -\frac{1}{2}\tan^{-1}\left[\frac{\frac{\alpha}{2\beta T^2}\left(\hat{C}_k^2 + \hat{S}_k^2\right)\sin\left[2\left(\gamma + \eta_k\right)\right]}{1 + \frac{\alpha}{2\beta T^2}\left(\hat{C}_k^2 + \hat{S}_k^2\right)\cos\left[2\left(\gamma + \eta_k\right)\right]}\right] \tag{49}$$

that deviates from the ideal lock point at $\phi_0 = 0$. The slope of Eq. (47) at the zero-crossing point of Eq. (49) can be found as

$$g'_{SC,k} = \sqrt{1 + \frac{\alpha}{\beta T^2}\left(\hat{C}_z^2 + \hat{S}_z^2\right)\cos\left[2\left(\gamma + \eta_k\right)\right] + \left(\frac{\alpha}{2\beta T^2}\left(\hat{C}_z^2 + \hat{S}_z^2\right)\right)^2} \tag{50}$$

On the other hand, the random part of the error feedback signal, Eq. (42), constitutes the effective noise as seen by the loop. Its variance is derived as

$$\sigma^2_{n_{eff},k} = \frac{S_L^{-1}}{2(E_b/N_0)}\left\{1 + \frac{\alpha}{2\beta T^2}S_L\left(\hat{C}_k^2 + \hat{S}_k^2\right)\left[1 + \frac{E_b}{N_0}\left(1 - \cos\left[2\big(2\phi_{0,k} + \gamma + \eta_k\big)\right]\right)\right]\right\} \tag{51}$$

where S_L is the squaring loss given in Eq. (29). From Eq. (51), an "instantaneous" loop SNR becomes

$$\rho_{\phi_c,k} = g'^2_{SC,k}\left(\frac{E_b/N_0}{B_L T}S_L\right)\left\{1 + \frac{\alpha}{2\beta T^2}S_L\left(\hat{C}_k^2 + \hat{S}_k^2\right)\left[1 + \frac{E_b}{N_0}\left(1 - \cos\left[2(2\phi_{0,k} + \gamma + \eta_k)\right]\right)\right]\right\}^{-1} \tag{52}$$

Again, this "instantaneous" loop SNR exists only for a loop with an infinitely small loop time constant.

Despite the unrealistic assumption of a loop with an infinitely small loop time constant, the instantaneous S-curve, carrier phase lock point, and loop SNR given in Eqs. (47), (49), and (52), respectively, provide good insight into how the carrier tracking loop responds to the presence of a chirp radar pulse. For example, Figs. 2 and 3 depict the change in the neighborhood of an impact event, which is defined as the time when the "instantaneous" radar frequency sweeps across the carrier frequency of the DSN telemetry signal. In Fig. 2, the instantaneous S-curve is plotted for three time periods—before, during, and after the impact event—when the peak interference-to-signal power ratio, α, is 3 dB. It clearly shows an S-curve in its transient state during the impact event as well as in its steady state before and after. In Fig. 3, the instantaneous carrier phase lock point and loop SNR loss are plotted against the symbol

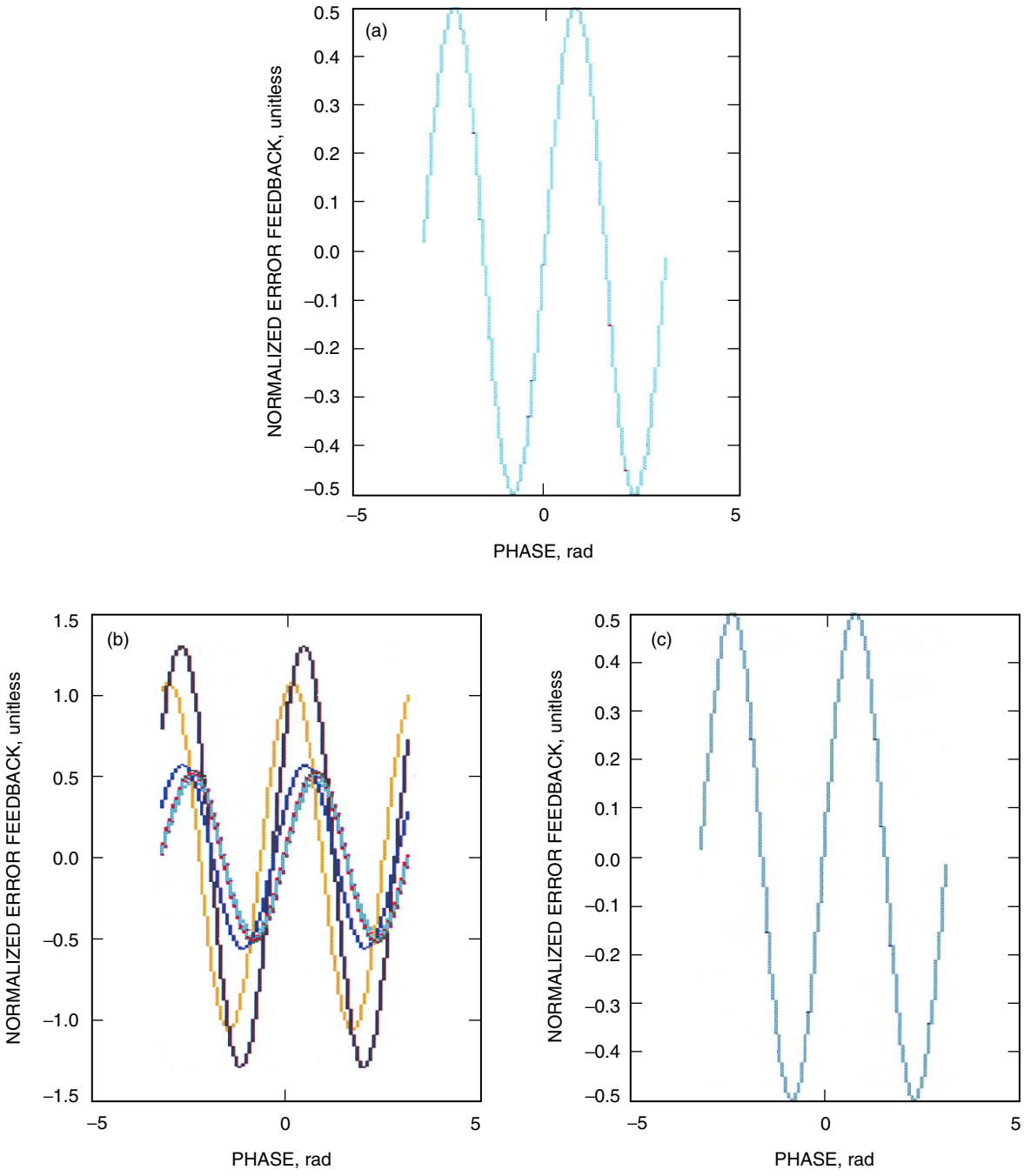

Fig. 2. Instantaneous S-curves (a) before, (b) during, and (c) after the impact event, when $\alpha = 3$ dB. (Note: each contains multiple slices at different times.)

index for the same peak interference-to-signal power ratio. With PRF = 4 kHz, $d = 40$ percent, $\Delta f = 0$, $T = 1$ μs, and $\beta = 0.5$ MHz/μs, the impact event affects carrier tracking for a short period of time (only a couple of symbols) around the mid-point of the radar pulse that covers 100 symbols. The existence of such an impact event for each chirp radar pulse also can be seen mathematically. It is found to be true that the term $\left(\hat{C}_k^2 + \hat{S}_k^2\right)$, which appeared before in equations such as Eq. (47) for the S-curve and Eq. (52) for the loop SNR, remains close to zero for most of the time except around the impact event. This indicates that only the symbols near the time when the instantaneous radar frequency sweeps across

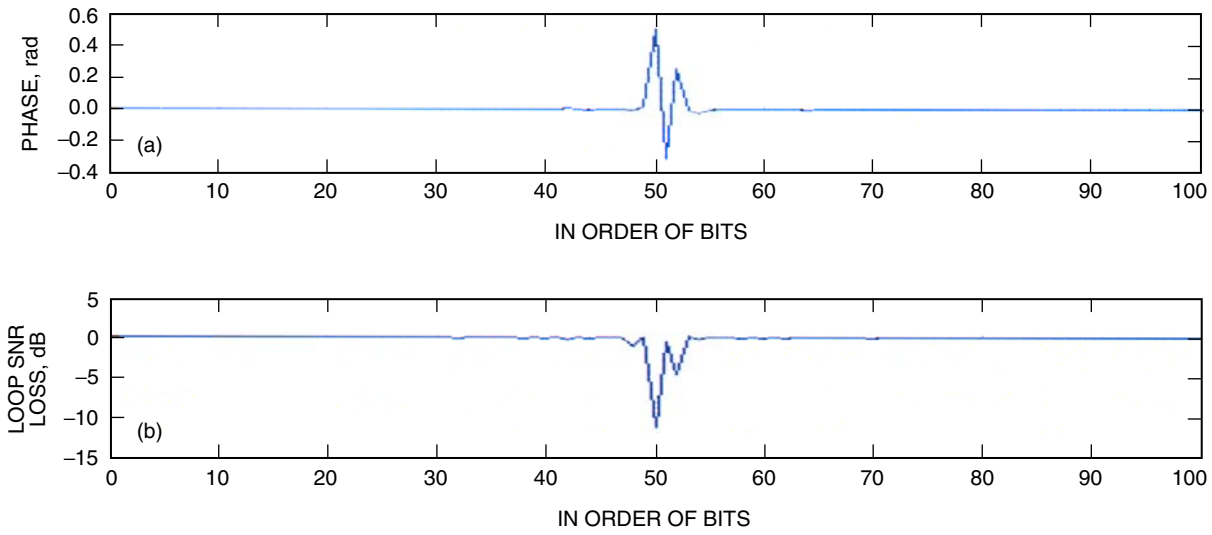

Fig. 3. Instantaneous (a) carrier phase lock point and (b) loop SNR loss when α = 3 dB.

the DSN's carrier frequency are subject to higher-than-normal bit-error probability. Other symbols, even within a radar pulse, are immune from the interference as long as they are not close to the impact event. It is important to note that, with a realistic loop bandwidth that satisfies $B_L T \ll 1$, the perturbation seen in these figures is to be averaged over the loop time constant, rendering a significantly smaller impact to the carrier tracking for cases with such a low peak interference-to-signal power ratio.

By factoring in the duty factor d of the radar pulse, one can obtain the time-averaged carrier phase lock point from Eq. (47) as

$$\phi_0 = -\frac{1}{2}\tan^{-1}\left[\frac{\frac{d\alpha}{2\beta T^2}M_x}{1+\frac{d\alpha}{2\beta T^2}M_0}\right] \tag{53}$$

and the time-averaged loop SNR from Eq. (51) as

$$\rho_{\phi_c} = \left(\frac{E_b/N_0}{B_L T}S_L\right)\left\{1+\frac{d\alpha}{2\beta T^2}S_L\left[M_1\left(1+\frac{E_b}{N_0}\right)+\left(\frac{E_b}{N_0}\right)\left(M_x\sin\left(4\phi_0\right)-M_0\cos\left(4\phi_0\right)\right)\right]\right\}^{-1} \tag{54}$$

where

$$\begin{aligned} M_1 &= \overline{\hat{C}_k^2+\hat{S}_k^2}^k \\ M_0 &= \overline{\left(\hat{C}_k^2-\hat{S}_k^2\right)}^k\cos\left(2\gamma\right)-2\overline{\hat{C}_k\hat{S}_k}^k\sin\left(2\gamma\right) \\ M_x &= \overline{\left(\hat{C}_k^2-\hat{S}_k^2\right)}^k\sin\left(2\gamma\right)+2\overline{\hat{C}_k\hat{S}_k}^k\cos\left(2\gamma\right) \end{aligned} \tag{55}$$

in which the over-line denotes an average over symbol index k. It is important to note that, with a realistic time constant, the carrier tracking loop would act in the time-averaged fashion under moderate interference. The carrier phase error again is modeled as a Tikhonov-distributed random variable with the probability density function

$$p(\phi_c\,|\gamma\,) = \frac{\exp\left(\frac{\rho_{\phi_c}}{4}\cos\left[2(\phi_c-\phi_0)\right]\right)}{\pi I_0\left(\frac{\rho_{\phi_c}}{4}\right)}, \quad |\phi_c| \le \frac{\pi}{2} \tag{56}$$

where ϕ_0 and ρ_{ϕ_c} are given in Eqs. (53) and (54), respectively.

C. Symbol Detection

The BPSK symbol (bit) detection is based on the output of the integrate-and-dump filter on the in-phase arm of the Costas loop. The normalized decision variable is found as

$$\begin{aligned}\frac{I_k}{\sqrt{P_d}T} &= d_k\cos\phi_c + \sqrt{\frac{\alpha}{2\beta T^2}}\left\{\cos\phi_c\left[\hat{C}_k\cos\gamma - \hat{S}_k\sin\gamma\right] - \sin\phi_c\left[\hat{C}_k\sin\gamma + \hat{S}_k\cos\gamma\right]\right\} + N_1 \\ &\triangleq u_k\left(\phi_c\right) + N_1\end{aligned} \tag{57}$$

Thus, for a given ϕ_c, the error probability for this particular symbol is

$$\begin{aligned}P_{b,k}(\phi_c\,|\gamma\,) &= \frac{1}{2}P_r\{u_k(\phi_c) < 0\,|d_k = 1\,\} + \frac{1}{2}P_r\{u_k(\phi_c) \ge 0\,|d_k = -1\,\} \\ &= \frac{1}{4}\mathrm{erfc}\left\{\sqrt{\frac{E_b}{N_0}}\left(\cos\phi_c + \sqrt{\frac{\alpha}{2\beta T^2}}\left[\hat{C}_k\cos\left(\phi_c+\gamma\right) - \hat{S}_k\sin\left(\phi_c+\gamma\right)\right]\right)\right\} \\ &\quad + \frac{1}{4}\mathrm{erfc}\left\{\sqrt{\frac{E_b}{N_0}}\left(\cos\phi_c - \sqrt{\frac{\alpha}{2\beta T^2}}\left[\hat{C}_k\cos\left(\phi_c+\gamma\right) - \hat{S}_k\sin\left(\phi_c+\gamma\right)\right]\right)\right\}\end{aligned} \tag{58}$$

and the unconditional bit-error probability for the kth symbol becomes

$$\begin{aligned}P_{b,k} &= \frac{1}{2\pi}\int_{-\pi}^{\pi} P_{b,k|\gamma}\,d\gamma \\ &= \frac{1}{2\pi}\int_{-\pi}^{\pi}\left(\int_{-\pi/2}^{\pi/2} P_{b,k}\left(\phi_c\,|\gamma\,\right)p\left(\phi_c\,|\gamma\,\right)d\phi_c\right)d\gamma\end{aligned} \tag{59}$$

With sufficiently large loop SNR such that the Tikhonov probability density function in Eq. (59) degenerates into a delta function at ϕ_0, the conditional bit-error probability for the kth symbol can be approximated by

$$P_{b,k|\gamma} = \frac{1}{4}\text{erfc}\left\{\sqrt{\frac{E_b}{N_0}}\left(\cos\phi_0 + \sqrt{\frac{\alpha}{2\beta T^2}}\left[\hat{C}_k\cos(\phi_0+\gamma) - \hat{S}_k\sin(\phi_0+\gamma)\right]\right)\right\}$$

$$+ \frac{1}{4}\text{erfc}\left\{\sqrt{\frac{E_b}{N_0}}\left(\cos\phi_0 - \sqrt{\frac{\alpha}{2\beta T^2}}\left[\hat{C}_k\cos(\phi_0+\gamma) - \hat{S}_k\sin(\phi_0+\gamma)\right]\right)\right\} \tag{60}$$

or, with η_k defined in Eq. (48),

$$P_{b,k|\gamma} = \frac{1}{4}\text{erfc}\left\{\sqrt{\frac{E_b}{N_0}}\left(\cos\phi_0 + \sqrt{\frac{\alpha}{2\beta T^2}\left(\hat{C}_k^2+\hat{S}_k^2\right)}\cos(\phi_0+\gamma+\eta_k)\right)\right\}$$

$$+ \frac{1}{4}\text{erfc}\left\{\sqrt{\frac{E_b}{N_0}}\left(\cos\phi_0 - \sqrt{\frac{\alpha}{2\beta T^2}\left(\hat{C}_k^2+\hat{S}_k^2\right)}\cos(\phi_0+\gamma+\eta_k)\right)\right\} \tag{61}$$

By setting $\alpha = 0$ in Eq. (61), one gets the bit-error probability for those symbols in the dead time of the pulsed interference as

$$P_b^* = \frac{1}{2}\text{erfc}\left(\sqrt{\frac{E_b}{N_0}}(\cos\phi_0)\right) \tag{62}$$

The overall BER is found as a duty-factor-weighted sum of two averaged bit-error probabilities: one for the symbols hit by the radar pulse and the other for the symbols in the dead time

$$P_b = d\overline{P_{b,k}}^k + (1-d)P_b^* \tag{63}$$

where $\overline{P_{b,k}}^k$ is an average of Eq. (59) over all symbols hit by the radar pulse.

IV. The Worst-Case Bit-Error Rate Performance

A. Fixed Symbol Rate

With the high tracking loop SNR approximation assumed, the BER curves for the low-rate (with $(\Delta f/\text{PRF}) \in \mathbb{Z}$) and the high-rate cases are plotted, with PRF = 4 kHz, d = 40 percent, $\Delta f = 0$, and $\beta = 0.5$ MHz/μs, for different interference-to-signal power ratios and bit rates. Figure 4 contains two plots for the low-rate cases: one for a bit rate of 10 b/s and the other for 1 kb/s, with a peak interference-to-signal power ratio ranging from 20 to 40 dB. As expected, the BER performance suffers more degradation under stronger interference. However, regardless of the bit rate, there is no difference between these two sets of curves, which, also affirmed by Eq. (34), demonstrates that the BER in this case has no explicit dependence on the bit rate for any given bit SNR.

For the high-rate case, four plots with bit rates of 50 kb/s, 100 kb/s, 500 kb/s, and 1 Mb/s are included in Fig. 5 for the same set of parameters used for the previous figure, except the range of the peak interference-to-signal power ratio is set from −6 to 9 dB. Unlike the low-rate case, the bit rate does play a role in the BER performance. It is clearly shown in Fig. 5 that, as bit rate increases, the BER performance is more sensitive to variation of the peak interference-to-signal power ratio. At higher rates,

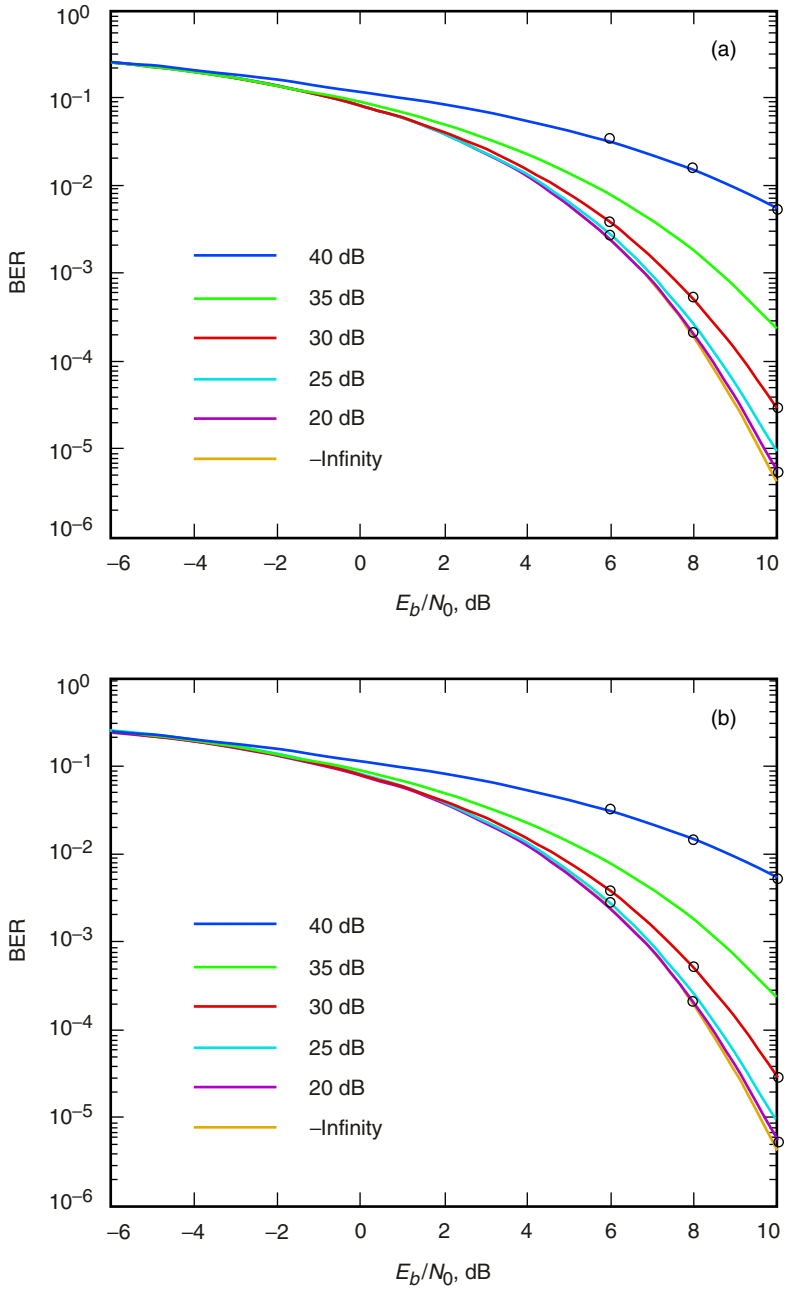

Fig. 4. BER curves for low-rate telemetry at (a) 10 b/s and (b) 1 kb/s. Circles are simulated points.

a BER performance floor starts to appear at a high bit SNR region where the detection errors caused by thermal noise are gradually diminishing. Virtually all of the errors in this region or beyond are now RFI-related, rendering a fixed BER level since the same percentage of bits is hit around an impact event regardless of how high the bit SNR is. This BER performance floor is settled at a level determined by the strength of the RFI. Figure 5 shows that, for a given peak interference-to-signal power ratio, the BER floor is higher (or appears earlier) for higher bit rates, since under this circumstance a higher bit rate at a fixed bit SNR implies a stronger RFI.

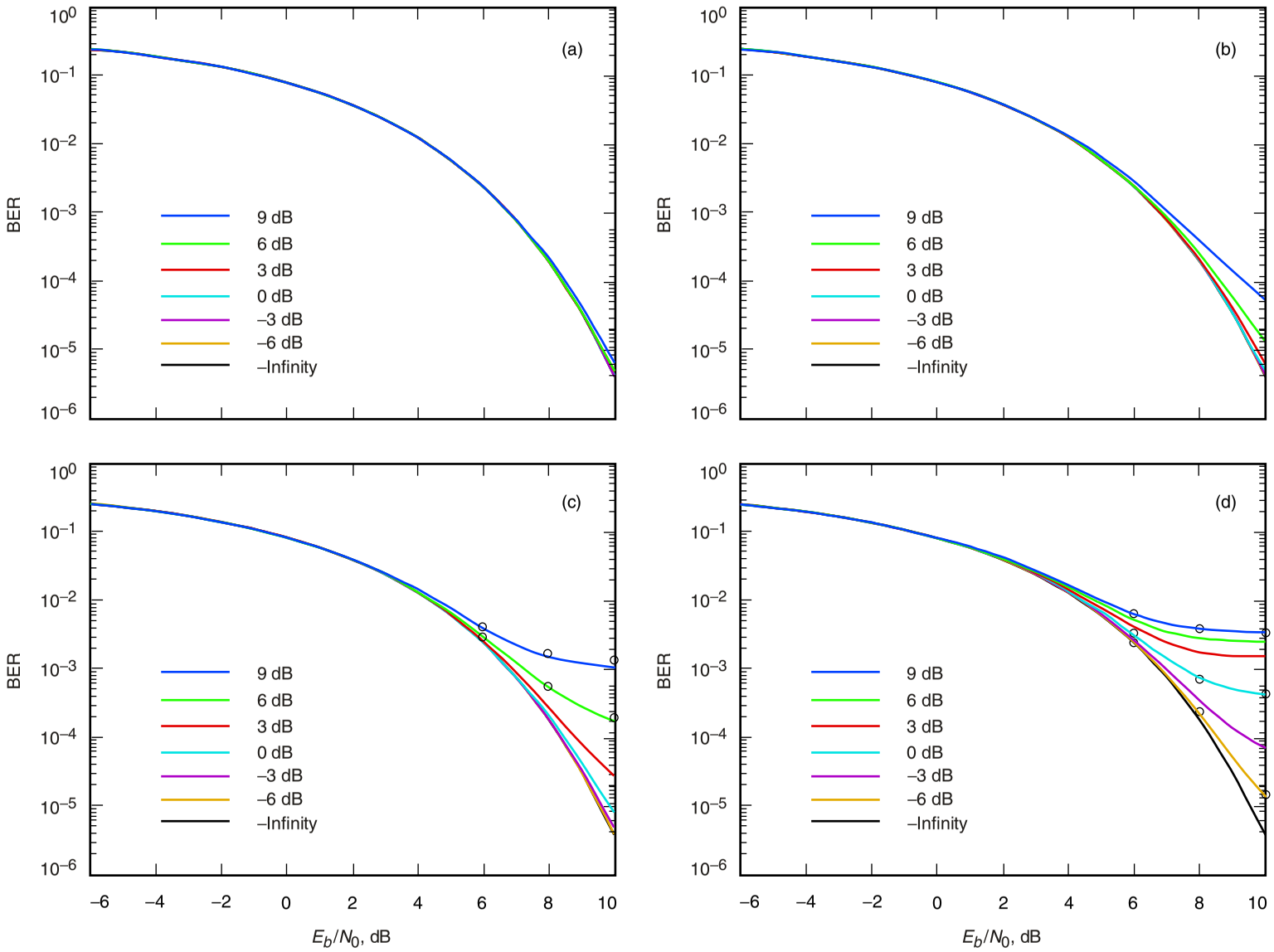

Fig. 5. BER curves for high-rate telemetry at bit rates of (a) 50 kb/s, (b) 100 kb/s, (c) 500 kb/s, and (d) 1 Mb/s. Circles are simulated points.

For the high-rate case, it is also important to examine the BER performance for the bits in the neighborhood of an impact event. These bits are under direct hit by an RFI pulse and are subject to much larger BER degradation than others. Since DSN telemetry is structured into frames and each frame has a frame header containing the critical information of the frame, there is a great risk that an entire frame will be lost if an RFI pulse collides with its frame header. Figure 6 shows a BER distribution for 10-Mb/s high-rate telemetry within a 1000-bit-long radar pulse.

The average BERs of the bits around the impact event and of all the bits are shown in Fig. 7 for comparison.

B. Fixed DSN Signal Power

When assessing the BER performance impact for a given DSN signal power level, one will keep P_d/N_0 at a constant level while changing E_b/N_0 via a change of bit rate. For the low-rate case, as indicated in Eq. (34), the set of BER curves remains the same as the one shown in Fig. 4, since the BER has no explicit dependence on the bit rate for any given bit SNR. For the high-rate cases, Fig. 8 shows two examples: one for a fixed $P_d/N_0 = 54$ dB-Hz and the other for $P_d/N_0 = 70$ dB-Hz. They look different, with the one for higher P_d/N_0 showing significant degradation with an increasing peak interference-to-signal power ratio while the other shows no degradation. The reason for such a contrast is the amount of background noise. It has been shown that the power spectral density of the pulsed-chirp RFI is much like a brick wall with a base equal to the width of the sweeping band and some ripple effect noticeable at the edges.[3]

In fact, the power spectral density level around the center of the RFI band is found as

$$S_0 \approx \frac{d(\alpha P_d)}{\beta\tau} = \frac{\alpha P_d}{\beta}\,(\mathrm{PRF}) \tag{64}$$

which is simply an average of the total power over its bandwidth. Comparing Eq. (64) to the background thermal noise, it is clear that the ratio of power spectral density level between the RFI and the noise is

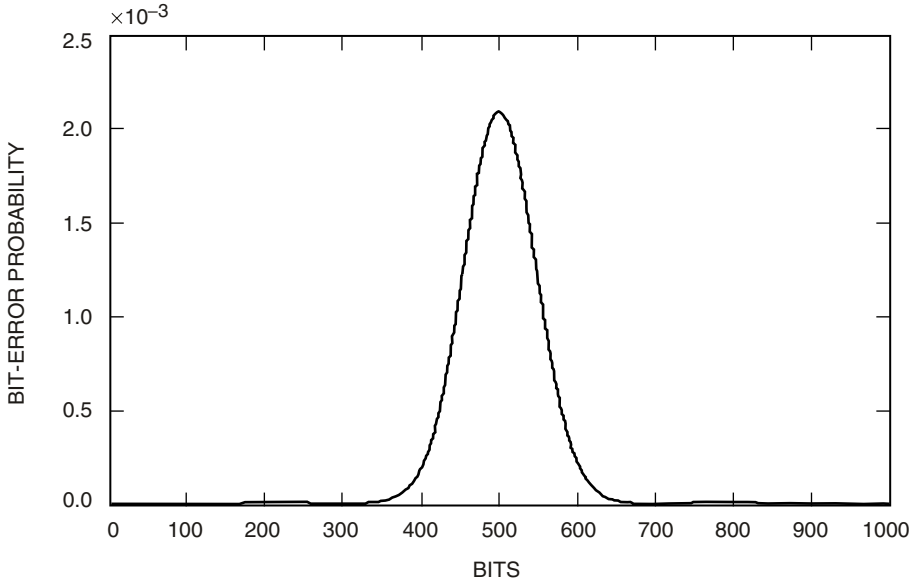

Fig. 6. A sample BER distribution within a radar pulse for high-rate telemetry at a bit rate of 10 Mb/s (PRF = 4 kHz, d = 40 percent, and α = –6 dB).

[3] P. Kinman, "Power Spectrum of Pulsed Radar Linear FM," Case Western Reserve University Memorandum 1239487-2, Cleveland, Ohio, May 1, 2002.

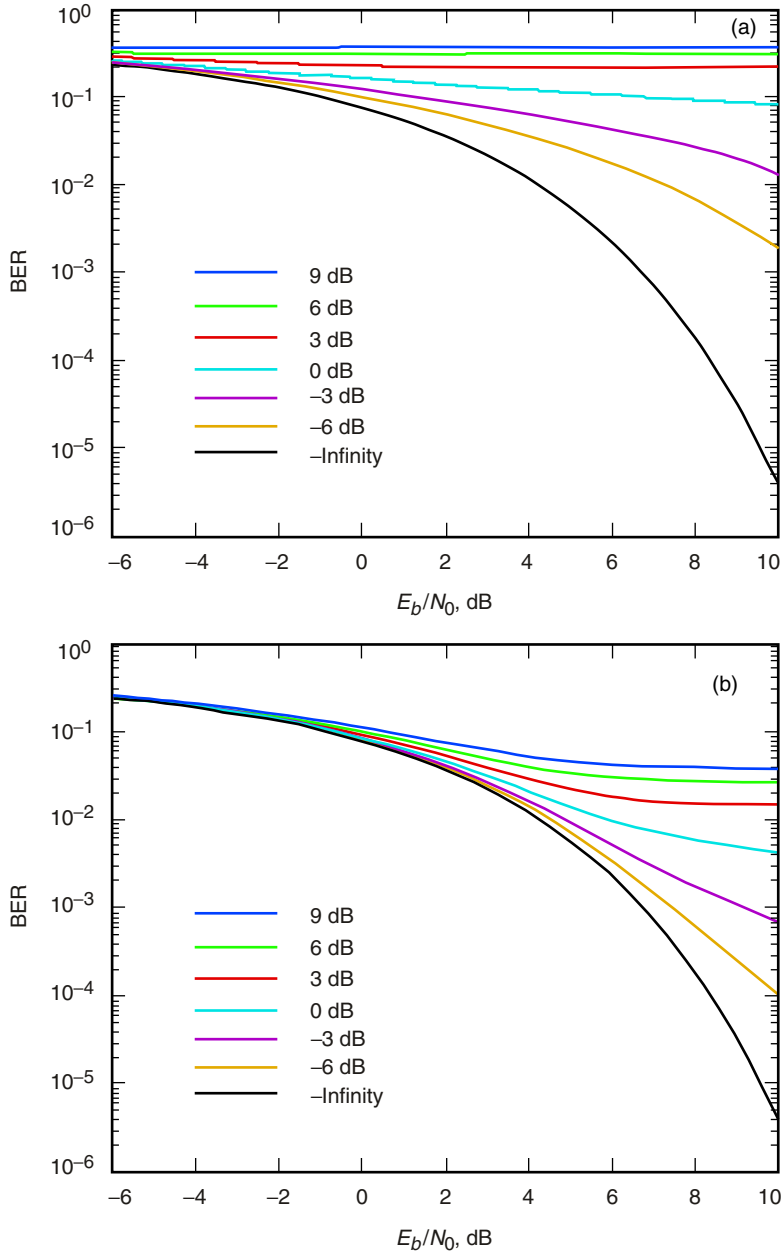

Fig. 7. BER curves for 10-Mb/s high-rate telemetry for (a) a 64-bit segment centered at the impact event and (b) all the bits.

$$S_r = \frac{2\alpha}{\beta}\,(\mathrm{PRF})\left(\frac{P_d}{N_0}\right) \tag{65}$$

When $S_r < 1$, the RFI is considered spectrally "buried" in the background noise. With the given α between -6 and 9 dB in this case, the RFI power spectral density level is 15 to 30 dB below that of the background noise when $P_d/N_0 = 54$ dB-Hz. As evidenced by the corresponding BER curves, no RFI-induced performance degradation can be seen for such a noise-dominant case. On the contrary, the RFI power spectral density level becomes 16 dB higher when P_d/N_0 is increased to 70 dB-Hz. This results in

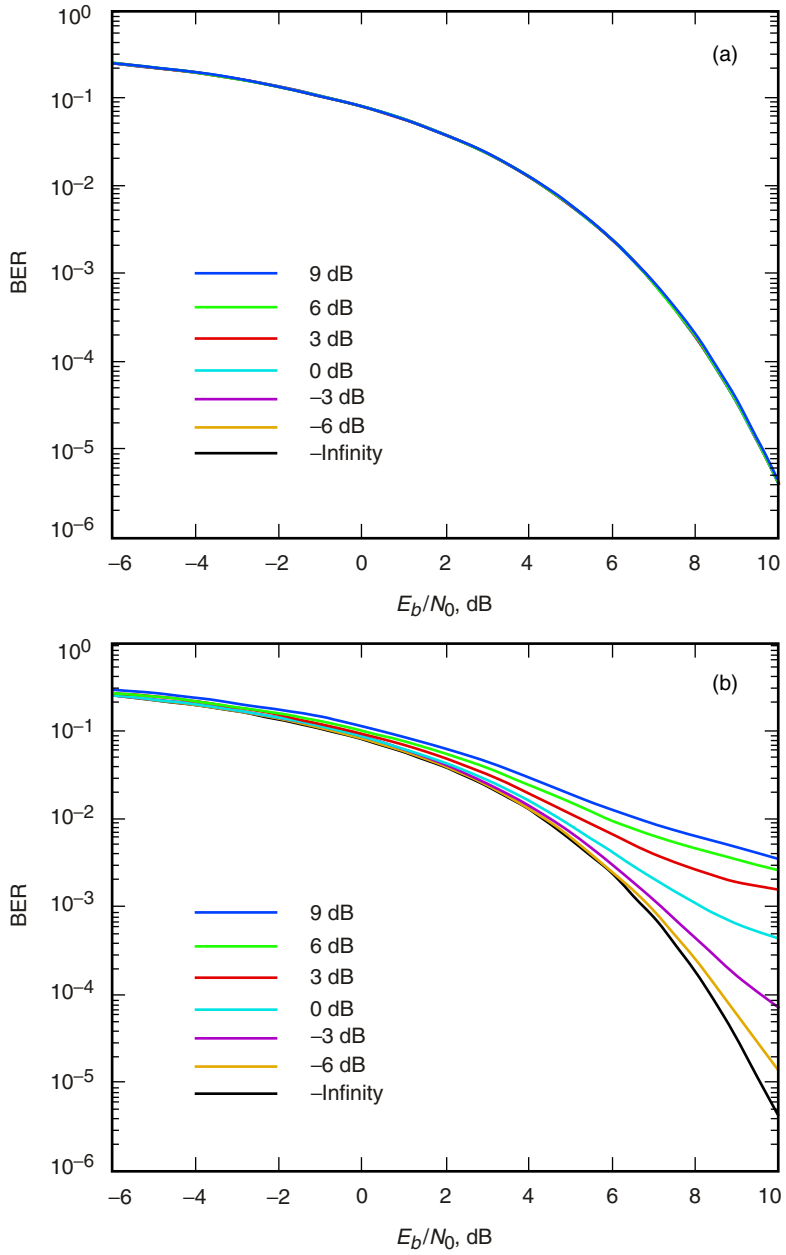

Fig. 8. BER curves for high-rate telemetry with fixed signal power for different P_d/N_0: (a) 54 dB-Hz and (b) 70 dB-Hz.

an RFI power spectral density level closer to or even slightly higher than that of the background noise. As such, the background noise is no longer the only dominant factor in determining the BER performance for this case.

Although the ratio of power spectral density level given in Eq. (65) does provide a rule of thumb about the risk of being affected by the pulsed-chirp RFI, and although it can be factored somehow into a BER formula, such as Eq. (34), for low-rate cases, it alone is not a tool for predicting how much the impact would be, especially for high-rate cases, where a relatively long-term observation such as the power spectral density is not that pertinent to the fast-paced receiver operation.

C. Fixed Interference Power

For a fixed interference power, the ratio

$$\frac{P_i}{N_0} = \frac{\alpha}{T}\left(\frac{E_b}{N_0}\right) \tag{66}$$

remains unchanged, and the BER given in Eq. (34) for the low-rate case with $(\Delta f/\mathrm{PRF}) \in \mathbb{Z}$ can be rewritten as

$$P_b\left(\phi_c\,|\lambda\right) = \frac{1}{4}\mathrm{erfc}\left\{\sqrt{\frac{E_b}{N_0}}\cos\phi_c + \sqrt{\frac{2P_iT}{\beta N_0}}\left(\frac{d}{\tau}\right)\left[C_z\cos\left(\phi_c+\lambda\right) - S_z\sin\left(\phi_c+\lambda\right)\right]\right\}$$

$$+\frac{1}{4}\mathrm{erfc}\left\{\sqrt{\frac{E_b}{N_0}}\cos\phi_c - \sqrt{\frac{2P_iT}{\beta N_0}}\left(\frac{d}{\tau}\right)\left[C_z\cos\left(\phi_c+\lambda\right) - S_z\sin\left(\phi_c+\lambda\right)\right]\right\} \tag{67}$$

In this case, with P_i/N_0 and E_b/N_0 fixed, an increase of symbol interval, T, enlarges the difference between the arguments of the two complementary error functions in Eq. (67) and, in turn, results in a higher BER. Therefore, the BER becomes higher as the symbol rate decreases.

As to the high-rate case, the BER given in Eq. (61) for a given bit hit by the radar pulse can be rewritten as

$$P_{b,k|\gamma} = \frac{1}{4}\mathrm{erfc}\left\{\sqrt{\frac{E_b}{N_0}}\cos\phi_0 + \sqrt{\frac{1}{2\beta T}\left(\frac{P_i}{N_0}\right)\left(\hat{C}_k^2+\hat{S}_k^2\right)}\cos\left(\phi_0+\gamma+\eta_k\right)\right\}$$

$$+\frac{1}{4}\mathrm{erfc}\left\{\sqrt{\frac{E_b}{N_0}}\cos\phi_0 - \sqrt{\frac{1}{2\beta T}\left(\frac{P_i}{N_0}\right)\left(\hat{C}_k^2+\hat{S}_k^2\right)}\cos\left(\phi_0+\gamma+\eta_k\right)\right\} \tag{68}$$

In this case, with P_i/N_0 and E_b/N_0 fixed, an increase of symbol rate stretches the difference between the arguments of these two complementary error functions and, therefore, results in a higher BER. Thus, the BER performance degrades further with an increasing symbol rate in the high-rate cases, which is contrary to the result for the low-rate cases.

V. Conclusion

This article documents an analysis of the bit-error performance of the coherent reception of a fully suppressed BPSK signal under in-band pulsed-chirp RFI. In this effort, as part of a study to assess the potential impact to the DSN operation from a synthetic-aperture radar project, two scenarios—one for low-rate and the other for high-rate telemetry—were studied, and analytical models were developed for each of them. For low-rate telemetry, the pulsed interference is effectively time-averaged by the tracking loop, rendering an interference behaving just like an additional loop noise that contributes to an increase of phase jitter. From this aspect, the impact to the carrier tracking in the low-rate case turns out to be fairly benign compared to the situation faced by high-rate telemetry. However, the RFI does have the potential to cause significant degradation to the receiver's hard detection on received symbols.

The pulsed nature of the interference plays an important role in the high-rate scenario. It creates periodic impact events, during which both carrier tracking and symbol detection are greatly affected.

Of these two crucial functions, it is likely the carrier tracking is able to withstand stronger interference because the loop's relatively long time constant usually provides sufficient time-average to smooth the impact out. Contrarily, the symbol detection is highly susceptible, especially when a slow frequency sweeping produces a prolonged impact event during which many symbols will be detected with errors. This results in a burst type of detection error happening periodically throughout the symbol sequence. Although certain error-correcting codes and bit-interleaving structures may help here, a direct hit happening to a critical part of the downlink stream, such as the frame header, will inevitably cause loss of data. In addition, a fairly high peak interference power can eventually force the carrier tracking loop out of lock, posing a great risk of losing telemetry data if they are not buffered.

In Figs. 4 and 5, the horizontal distance between the reference curve and the curve for a given peak interference-to-signal power ratio is the required amount of additional signal power (in decibels) to compensate for the RFI impact. It is referred to as the radio loss at a specific BER level. In the low E_b/N_0 region (e.g., 0 dB or lower), it is found through numerical evaluation that a radio loss of 0.1 dB or higher would occur when the peak interference-to-signal power ratio is around 30 dB for the low-rate ($\sim$1 kb/s), 18 dB for the medium-rate ($\sim$50 kb/s), and 3 dB for the high-rate ($\sim$1 Mb/s) cases. In order to avoid risk to DSN operations, it is strongly recommended that the peak interference-to-signal power ratio be restricted below these levels, such that the radio loss caused by the pulsed radar operation will not exceed 0.1 dB.

Reference

[1] W. C. Lindsey, *Synchronization Systems in Communication and Control*, Englewood Cliffs, New Jersey: Prentice-Hall, 1972.